

Framework-solvent interactional mechanism and effect of NMP/DMF on solvothermal synthesis of $[\text{Zn}_4\text{O}(\text{BDC})_3]_8$

Zheng-ping WU^{1,2}, Ming-xue WANG¹, Li-jiao ZHOU¹,
Zhou-lan YIN^{1,2}, Jin TAN¹, Jin-ling ZHANG¹, Qi-yuan CHEN^{1,2}

1. School of Chemistry and Chemical Engineering, Central South University, Changsha 410083, China;

2. Key Laboratory of Resource Chemistry of Nonferrous Metals, Ministry of Education, Central South University, Changsha 410083, China

Received 12 November 2013; accepted 11 March 2014

Abstract: In order to explore the effect mechanism of solvent on the synthesis of the metal organic framework materials, the microscopic interaction between solvent and framework and the effects of N,N-dimethyl-formamide (DMF) or N-methyl-2-pyrrolidone (NMP) on solvothermal synthesis of $[\text{Zn}_4\text{O}(\text{BDC})_3]_8$ were investigated through a combined DFT and experimental study. XRD and SEM showed that the absorbability of NMP in the pore of $[\text{Zn}_4\text{O}(\text{BDC})_3]_8$ was weaker than that of DMF. The thermal decomposition temperature of $[\text{Zn}_4\text{O}(\text{BDC})_3]_8$ synthesized in DMF was higher than that in NMP according to TG and FT-IR. In addition, the nitrogen sorption isotherms indicated that NMP improved gas sorption property of $[\text{Zn}_4\text{O}(\text{BDC})_3]_8$. The COSMO optimized calculations indicated that the total energy of $\text{Zn}_4\text{O}(\text{BDC})_3$ in NMP was higher than that in DMF, and compared with non-solvent system, the charge of zinc atoms decreased and the charge value was the smallest in NMP. Furthermore, the interaction of DMF, NMP or DEF in $[\text{Zn}_4\text{O}(\text{BDC})_3]_8$ crystal model was calculated by DFT method. The results suggested that NMP should be easier to be removed from pore of materials than DMF from the point of view of energy state. It can be concluded that NMP was a favorable solvent to synthesize $[\text{Zn}_4\text{O}(\text{BDC})_3]_8$ and the microscopic mechanism was that the binding force between $\text{Zn}_4\text{O}(\text{BDC})_3$ and NMP molecule was weaker than DMF.

Key words: solvothermal synthesis; $[\text{Zn}_4\text{O}(\text{BDC})_3]_8$; N-methyl-2-pyrrolidone; interactional mechanism; COSMO solvation model; density functional method

1 Introduction

How to select favourable solvent is one of the key questions that should be thought about when any kind of the metal organic framework materials (MOFs) is constructed [1–3]. There are several popular acceptable opinions about the main functions of solvent: deprotonating function on carboxylic acid ligand, promotion of the reactions which are difficult to proceed in aqueous solution due to the ability of solubilizing reactants, obtaining better crystalline materials, being conducive to form the porous structure in frameworks as template. For the purpose to avoid interrupting or participating in synthesized process, the co-ordination trend of solvent should be weaker than that of carboxylic acid ligand. N,N-dimethylformamide(DMF) was the

most common solvent and triethylamine (TEA), N,N-diethyl formamide (DEF) and N-methyl-2-pyrrolidone (NMP) were also usually used as solvents [4–6]. Although it was accepted that the solvents not only acted as general solvents but also intervened the self-assembly reaction of MOFs, the mechanism of solvent is not explained clearly until now.

MOF-5 is typical MOFs material reported by LI et al [7] firstly and the hot research topics in this field included porous structure analysis, catalyst supported property and gas adsorption of MOF-5, etc., recently in China [8–10]. In many cases, DMF was the most widely applied solvent. LI and YANG [11] and CHENG et al [12] synthesized MOF-5 in DMF solvent, studied morphology control, and significantly enhanced hydrogen storage in MOF-5 respectively. MOF-5 membranes were synthesized, characterized and

concentrated on its transport properties in DMF by ZHAO et al [13]. KIM et al [14] synthesized the interpenetrated structure MOF-5 in DMF solvent, and studied the effect of pH on change of structure and property of hydrogen storage.

DEF and NMP were rarely reported using as solvents in synthesizing MOF-5. For instance, MOF-5 was prepared in DEF by ROSI et al [15,16] and SABO et al [17], whose research purposes were to characterize the properties of hydrogen storage [15], infinite secondary building units, forbidden catenation in MOFs [16] and the effect of palladium modified on the specific surface area [17] of MOF-5 respectively. ZHANG and HU [18] investigated the difference of DMF sorption on the $Zn_4O(C_8H_4O_4)_3$ framework synthesized in DMF and DEF. SON et al [19], LU et al [20] and LEE and PARK [21] reported solvent NMP which was selected to synthesize MOF-5. Although the synthesized mechanism of MOFs was also discussed in Refs. [22–25], the reaction mechanism and effect of DMF, NMP and DEF solvents were difficult to make clear because the synthesis processes were self-assemble and usually proceeded in sealed containers, which was the reason why we tried to use experimental and theoretic methods to investigate the solvent effect and reaction mechanism.

In this work, based on the experimental results, the effect of solvent molecules on the framework structure were explored in an unique way for the first time, which was combined with two different angles of views: one was molecule level, using COSMO models to reveal the difference of microscopic properties of structure unit $Zn_4O(BDC)_3$ in different solvents, and another was putting the solvent molecule in the channel of MOF-5 crystal model, simulating the interactions between solvent and framework. Through this study, not only the effects of solvent and the interactional mechanism between solvent and framework were clarified by XRD, SEM, TG, FT-IR, nitrogen sorption isotherms and DFT methods, but also a new combinational research path was provided to understand the self-assemble crystallization process mechanism better.

2 Experimental

2.1 Reagent and equipments

The solvothermal reactions were carried out in Teflon-lined autoclave. All reagents were purchased from commercial sources and used without further purification. $Zn(NO_3)_2 \cdot 6H_2O$ (Analytical reagent), terephthalic acid ($\geq 99.0\%$), N-methyl-2-pyrrolidone was (Chemical reagent), N,N-dimethylformamide (Analytical reagent), dichloromethane (Analytical reagent) were purchased from Xilong Chemical Co., Ltd., National

Chemical Group Co., Ltd., Shanghai Shunqiang Chemical Co., Ltd. and Tianjin Fuyu Fine Chemical Co., Ltd., respectively.

The powder X-ray diffraction (XRD) patterns were recorded on a Rigaku 2500 diffractometer equipped with a sealed Cu tube. SEM images were characterized with Nova Nano SEM 230 scanning electron microscope (SEM). IR spectra were determined at room temperature with Nico LET-6700 FT-IR and the thermogravimetric analysis (TG) data were obtained on Thermo TG/FT-IR in nitrogen atmosphere (70 mL/min) at a constant rate of 5 °C/min from 25 to 600 °C. The nitrogen sorption isotherm at 77 K was volumetrically measured up to 10^5 Pa by the auto-sorb 1MP instrument by micro-meritics ASAP2020.

2.2 Solvothermal synthesis

$Zn(NO_3)_2 \cdot 6H_2O$ (1.350 g) and H_2BDC (0.249 g) were dispersed in DMF (49 mL) under ultrasound, then heated at 120 °C for 24 h in a Teflon-lined autoclave. The precipitate was collected by vacuum filtration, washed with DMF, soaked in dichloromethane and dried in vacuum drying oven at 120 °C for 24 h. This precipitate was named as MOF-5_DMF. Using the same approach, replacing DMF with NMP (50 mL), the crystalline precipitate was named as MOF-5_NMP.

Two samples of newly-made precipitate of MOF-5_NMP were soaked in NMP and DMF for 24 h respectively, then soaked in dichloromethane and dried in vacuum drying oven at 120 °C. These two products were named as MOF-5_NMP-N and MOF-5_NMP-D, in which '-N' means -NMP and '-D' means DMF.

3 Results and discussion

3.1 XRD and TEM analysis

Four characteristic peaks at $2\theta=6.8^\circ$, 9.7° , 13.7° and 15.4° confirmed that the MOF-5 crystalline products (b), (c), (d) and (e) were pure phase by XRD analysis (see Fig. 1). The intensity ratio of the XRD peak at 9.7° to the peak at 6.8° (referred to as the $R1$ value) could predict the adsorption properties of MOF-5 material: the lower the intensity ratio was, the more porous the material was [26–30]. A high $R2$ value (the ratio of the intensity of the peak at 13.8° to that at 6.8°) suggested that it was an interpenetrated structure, especially when the $R1$ value was low [6–8,14]. The $R1$ value of MOF-5_NMP was 0.291 that was closed to the standard value (0.202) and the $R2$ value was lower than $R1$, which meant that the utilization of porous substance of MOF-5_NMP was high and MOF-5_NMP was an ideal non-penetrated MOF-5 material. The $R1$ value (1.224) of MOF-5_DMF was higher than that of MOF-5_standard instead, which implied that MOF-5_DMF had a low surface area and

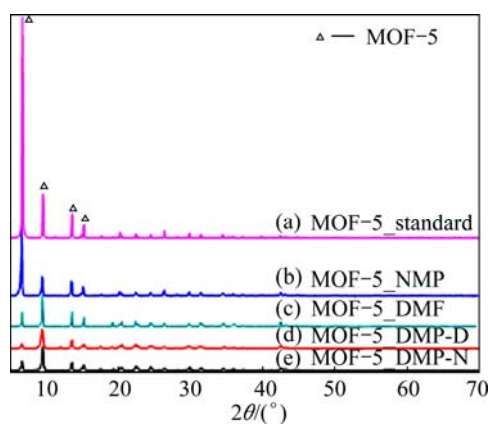


Fig. 1 XRD patterns of samples

small porous relatively. It might be some solvent molecules or zinc species entrapped in the MOF-5 framework.

The $R1$ values of MOF-5_NMP-D and MOF-5_NMP-N were 2.2 and 4, which were far higher than that of MOF-5_NMP (0.291), and the peak intensity at 9.7° was extremely high. That was to say that there might be more guest molecules in frameworks after being soaked in solvent for 24 h and then dried in vacuum drying oven at 120°C for 24 h. Also $R1$ value of MOF-5_NMP-D was far higher than that of MOF-5_NMP-N, which confirmed that NMP was easier

to remove from pore channel than DMF.

SEM images of MOF-5_NMP and MOF-5_DMF (see Fig. 2) showed that the precipitates were all non-interpenetrated cubic-like crystals and the sizes were similar, but the differences in characteristics of crystal surface and appearance were that MOF-5_NMP presented quite smooth surface and completed crystalline feature, which was coincidence with the XRD analysis results. Comparably, the cubic crystal of MOF-5_DMF was imperfect and the degree of crystallinity was lower than that of MOF-5_NMP. It could be seen apparently that there were some fissures on the surface of MOF-5_DMF crystal. All these results suggested that NMP was a favourable solvent to synthesize MOF-5 material compared with DMF.

It also could be seen in Fig. 2 that MOF-5_NMP-N and MOF-5_NMP-D still kept stable framework, smooth surface and non-interpenetrated structure, which implied that the effect of being soaked in NMP or DMF and then dried at 120°C was not obvious interrupting on the appearance of MOF-5.

3.2 Thermogravimetric analysis

TG curves (see Fig. 3) indicated that the decomposition temperatures of MOF-5_NMP, MOF-5_NMP-N and MOF-5_NMP-D were $425\text{--}525^\circ\text{C}$; however, MOF-5_DMF started to decompose at

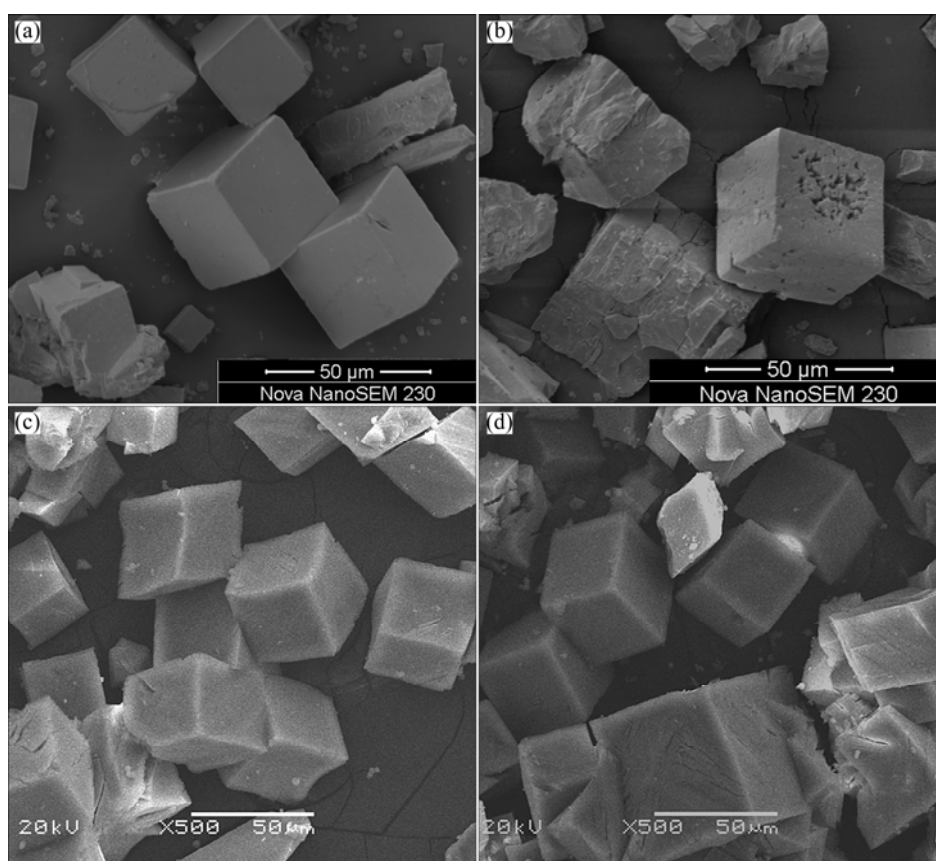


Fig. 2 SEM images of four samples: (a) MOF-5_NMP; (b) MOF-5_DMF; (c) MOF-5_NMP-D; (d) MOF-5_NMP-N

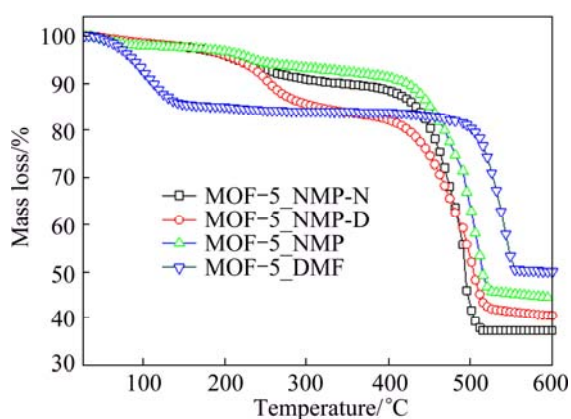


Fig. 3 TG curves of four samples

475 °C and was completely break down at 550 °C. The thermal stability of MOF-5 materials was reduced when NMP was used as solvent instead of DMF. Being soaked in NMP or DMF and then dried at 120 °C would not change the decomposed temperature of the products obviously. The mass process from 200 °C to 300 °C implied that DMF molecular in pore canal was more difficult to remove than NMP.

3.3 FT-IR spectroscopy analysis

The FT-IR spectroscopy analysis (see Fig. 4) of MOF-5 materials showed that there were three mainly regions: in 3500–3300 cm^{-1} region, a broad band was the characteristic peak of water absorbed during measurement process; in 1600–1300 cm^{-1} , 1610–1550 cm^{-1} and 1420–1300 cm^{-1} region, two strong peaks characterized symmetry and antisymmetry absorption peaks of —COOH in H_2BDC respectively; in 1300–650 cm^{-1} region, the out-of-plane and in-of-plane C—H bending characteristic peaks appeared, which were characteristic absorption peaks of MOF-5 framework structure. Additionally, MOF-5_NMP-D and MOF-

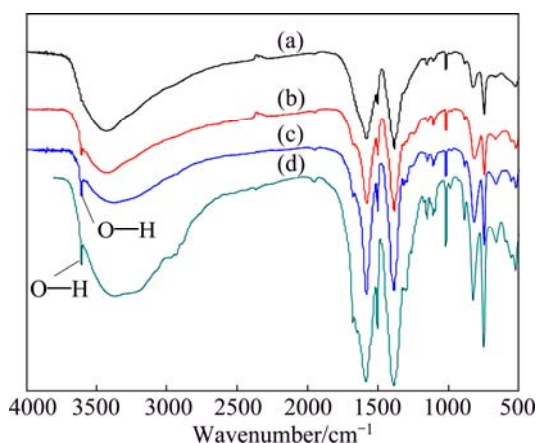


Fig. 4 FT-IR spectroscopy analysis of four samples: (a) MOF-5_NMP; (b) MOF-5_DMF; (c) MOF-5_NMP-N; (d) MOF-5_NMP-D

5_NMP-N had some absorption peaks at 3606 cm^{-1} , which indicated that the bending motions of the O—H bonds should exist, and the reason could be explained that there was trace water in solvent which might bond with MOF-5 framework in some ways because of being soaked in NMP or DMF for a long time.

3.4 DTG-FT-IR analysis

DTG-FT-IR results (see Fig. 5) were coincident with TG analysis. Three strong adsorption peaks at 625–700 cm^{-1} , 2220–2400 cm^{-1} and 3000 cm^{-1} of MOF-5_DMF and MOF-5_NMP existed in 90–110 min (measurement temperature 25–600 °C, 5 °C/min, corresponding temperature 475–550 °C) and 80–100 min (corresponding temperature 425–525 °C). More specific DTG-FT-IR results at 90 and 102 min showed the difference decomposition characters of these two MOF-5 materials, and the thermal stability of MOF-5_DMF was higher than that of MOF-5_NMP.

3.5 Gas adsorption/desorption analysis

Nitrogen adsorption-desorption curves (see Fig. 6) showed type-I behaviour of the six samples. The Langmuir surface areas of MOF-5_NMP and MOF-5_DMF estimated by nitrogen sorption isotherms are 1071 and 952 cm^2/g respectively, which meant that the material prepared using NMP solvent would be favourable to improve gas sorption property of MOF-5. According to the Langmuir surface area of MOF-5_NMP-N and MOF-5_NMP-D shown in Fig. 6, clearing solvent away was one of the key factors to synthesize MOF-5 materials with better gas sorption property. The reason why the samples soaked in solvent and then dried in vacuum drying oven had a relatively small Langmuir surface area was that the soaking process might make some solvent molecules leave in frameworks even after being dried. The Langmuir surface area of MOF-5_NMP-N was higher than that of MOF-5_NMP-D, which confirmed that NMP was easier to take out from MOF-5 framework than DMF.

3.6 COSMO optimization calculations on interactional systems of $\text{Zn}_4\text{O}(\text{BDC})_3$ and solvents

Although the effects of solvent on the properties of MOF-5 synthesized in DMF and NMP were studied using XRD, SEM, TG and FT-IR, the microscopic effect mechanism of solvent on the properties of MOF-5 still needed to be investigated in depth. Based on this, three different solvents, DMF, NMP and DEF were selected as representative solvents, and the interaction between secondary structure unit of MOF-5 and three different solvents was studied using DMol3 program based on the density functional theory.

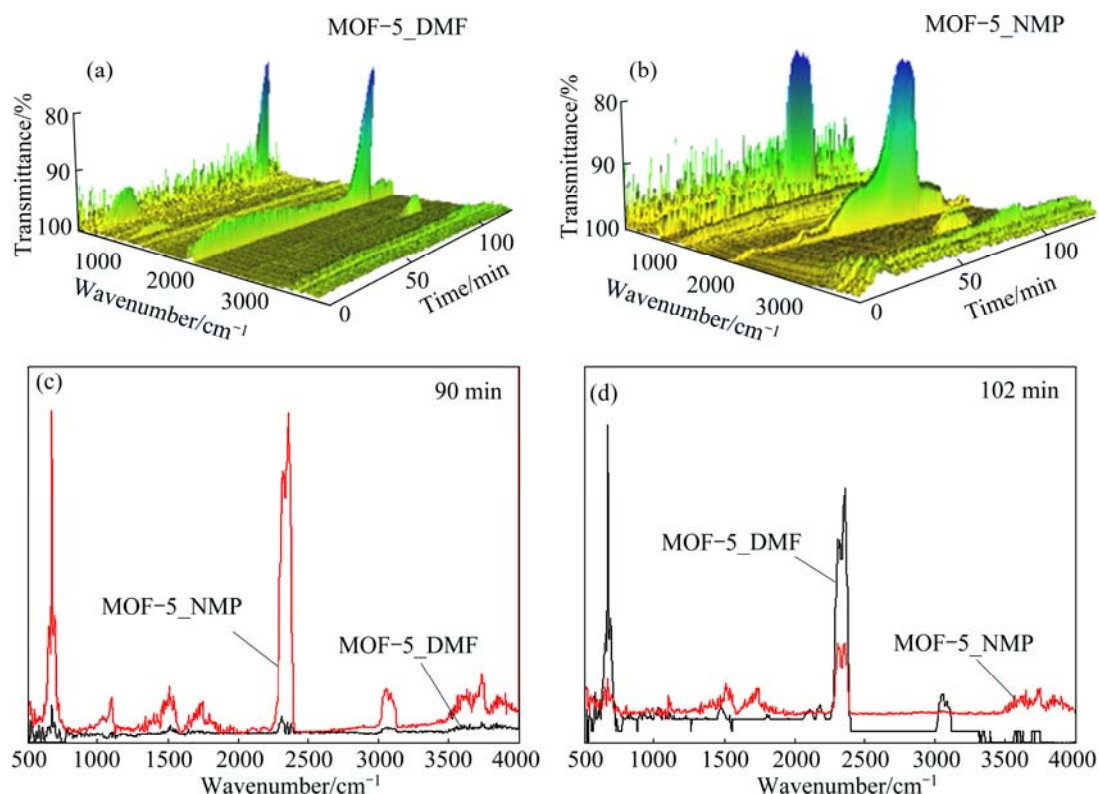


Fig. 5 DTG-FT-IR analysis results of MOF-5_DMF and MOF-5_NMP

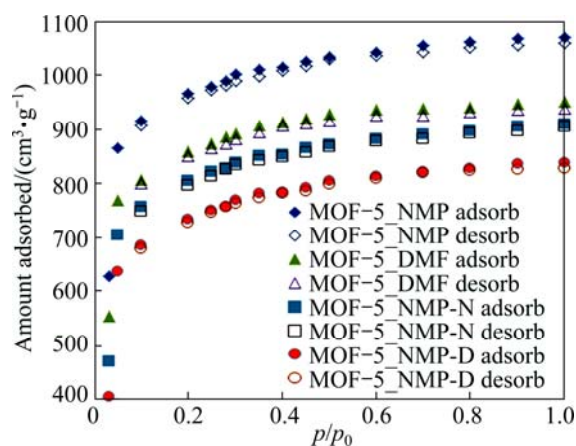


Fig. 6 Nitrogen sorption isotherms of MOF-5 materials at 77 K (Filled circles: sorption; open circles: desorption. p/p_0 is the ratio of gas pressure (p) to saturation pressure (p_0))

The secondary structure units of $Zn_4O(BDC)_3$, DMF, NMP and DEF were built (see Fig. 7) respectively. The COSMO solvation model is shown in Fig. 8. 32.2 and 36.6 are dielectric constant values of NMP and DMP which were set as solvent parameter respectively when performing the DMol3 calculations. Figure 9 shows the interactional models of $Zn_4O(BDC)_3$ and DEF as an example of two typical models due to the relative orientation of solvent molecular and $Zn_4O(BDC)_3$. There were two interactional models according to the relevant situation of C=O bond of DEF. The model was named

as Zn4-DEF-1 when the C=O bond was far away from Zn group of $Zn_4O(BDC)_3$; otherwise, named as Zn4-DEF-2. Using the same representation, Zn4 presented $Zn_4O(BDC)_3$, 1 and 2 presented C=O bond which was far away from or closed to Zn4 group respectively; the other four models were named as Zn4-DMF-1, Zn4-DMF-2, Zn4-NMP-1 and Zn4-NMP-2.

Continuum solvation model (COSMO) was used to investigate solvent effect by DMol3 based on the DFT method [31–35]. The COSMO optimization calculations were implemented and the convergence thresholds sets of energy value, the max force and max displacement were 4.36×10^{-23} J, 8.72×10^{-21} J/Å and 0.005 Å respectively. The solute molecule $Zn_4O(BDC)_3$ formed a cavity within the dielectric continuum of permittivity, ϵ . In this work, the experimental dielectric constants of DMF and NMP were set as 36.7 and 32.2.

The COSMO energy calculation results showed that the total energy of $Zn_4O(BDC)_3$ setting NMP dielectric constant as solvation model parameter was higher than DMF and the difference value was 8.6405 kJ/mol, which meant that the bonding force between $Zn_4O(BDC)_3$ and DMF molecule was stronger. The Mulliken atomic charges of zinc and oxygen are listed in Table 1 and the effect of solvent on atomic charge calculation results was obvious. Compared with non-solvent system, the charges of four zinc atoms decreased in some degree and the charge value was the smallest in NMP basically. Charge

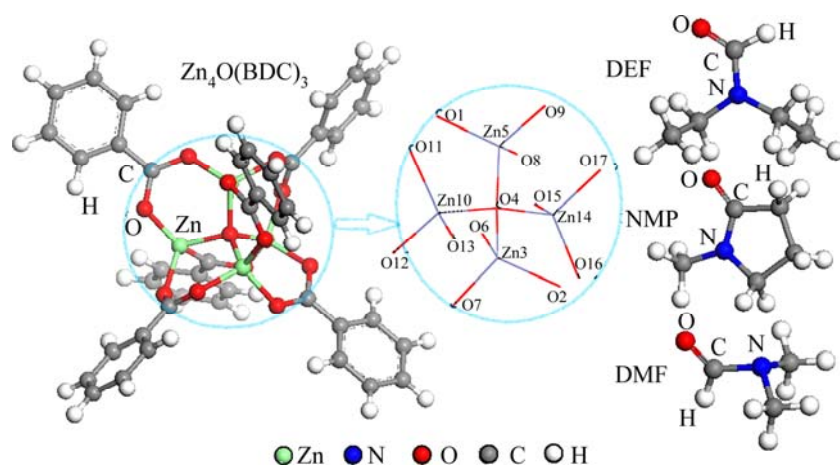


Fig. 7 Structure models of $Zn_4O(BDC)_3$, DMF, NMP and DEF



Fig. 8 COSMO solvation model of $Zn_4O(BDC)_3$

value of all oxygen atoms decreased from -0.61 to -0.57 except the centre oxygen atom O4. The charge of O4 was -1.064 and its absolute value was far larger than the other twelve oxygen atoms that belong to zinc tetrahedral. This indicated that the ionic between zinc and oxygen reduced, and in other words, the covalent might be strengthened because of the effect of solvent.

Furthermore, the frequency calculation results of the total energy and Mulliken atomic electrostatic charge were analyzed.

The energy state of $Zn_4O(BDC)_3$ and the same solvent reaction systems was different due to the different relative orientation of the solvent molecule. The energy value order of the same solvent systems were: $E_{(Zn_4-DMF-1)} > E_{(Zn_4-DMF-2)}$, $E_{(Zn_4-NMP-1)} < E_{(Zn_4-NMP-2)}$ and $E_{(Zn_4-DEF-1)} < E_{(Zn_4-DEF-2)}$, which inferred that NMP and DEF were easy to move out from the corresponding MOF-5 framework when the $C=O$ bond was close to Zn group of $Zn_4O(BDC)_3$ because of the relative high energy state. Instead, DMF molecular would be easy to remove in DMF and $Zn_4O(BDC)_3$ systems when the

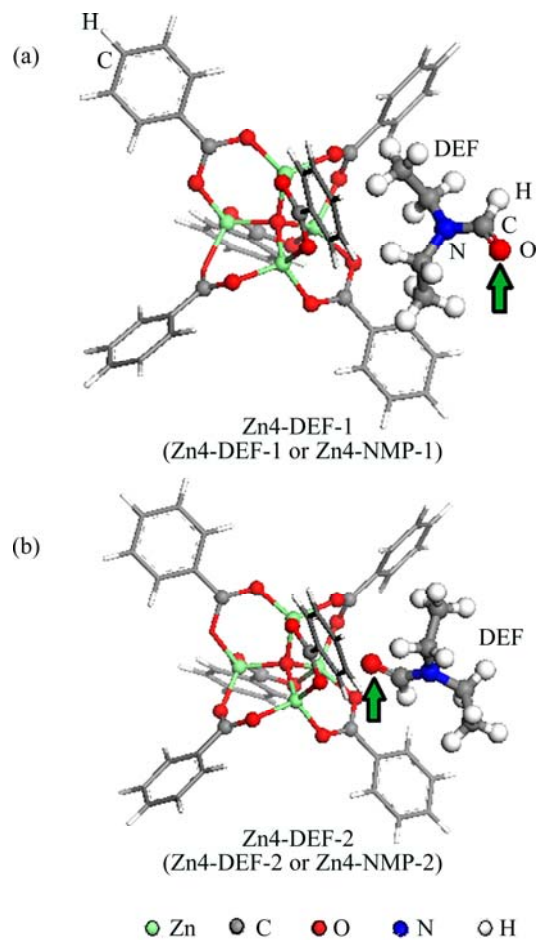


Fig. 9 Interactional structure models of $Zn_4O(BDC)_3$ with DMF, NMP or DEF

$C=O$ bond was far away from Zn group of $Zn_4O(BDC)_3$.

Absolute values of total energy difference, $|\Delta E_{[(Zn_4-DMF-2)-(Zn_4-DMF-1)]}|$, $|\Delta E_{[(Zn_4-NMP-2)-(Zn_4-NMP-1)]}|$ and $|\Delta E_{[(Zn_4-DEF-2)-(Zn_4-DEF-1)]}|$ were 95.3, 578.1 and 48.8 kJ/mol, respectively, which suggested that the effect of $C=O$ situation of NMP on the energy state was more

significant than DMF or DEF system. On other point of view of the relative energy state, the effect of difference situations of C=O bond on the energy state of Zn4-NMP was more distinct than the other two interactional models, which implied that C=O bond of NMP molecule had a tendency to be farther away from Zn group of $Zn_4O(BDC)_3$ than that of DMP or DEF.

Table 1 Mulliken atomic charges of zinc and oxygen

Atom	Non-solvent	DMF	NMP
Zn3	1.092	1.001	0.995
O2	-0.611	-0.570	-0.570
O6	-0.611	-0.574	-0.574
O7	-0.610	-0.573	-0.572
O4	-1.064	-0.865	-0.864
Zn5	1.092	1.012	1.002
O1	-0.610	-0.575	-0.576
O8	-0.612	-0.574	-0.572
O9	-0.612	-0.576	-0.577
O4	-1.064	-0.865	-0.864
Zn10	1.092	1.006	1.014
O11	-0.612	-0.570	-0.573
O12	-0.611	-0.574	-0.574
O13	-0.611	-0.577	-0.579
O4	-1.064	-0.865	-0.864
Zn14	1.092	1.000	0.992
O15	-0.611	-0.583	-0.580
O16	-0.611	-0.574	-0.574
O17	-0.611	-0.577	-0.577
O4	-1.064	-0.865	-0.864

Mulliken atomic electrostatic charges of four zinc atoms in six $Zn_4O(BDC)_3$ and DMF, NMP or DEF interactional systems are shown in Fig. 10. Zinc atomic electrostatic charges in $Zn_4O(BDC)_3$ are also marked in Fig. 11 for comparison. The atomic electrostatic charge of the No.3 zinc atom was similar and the effect of zinc atomic electrostatic charge on DMF interactional system was definitely smaller than the other two systems. Three

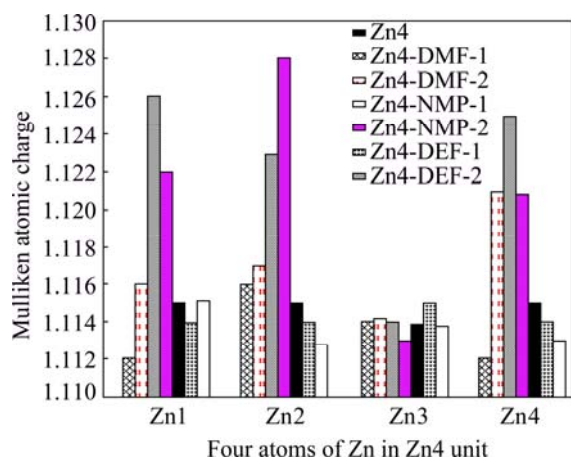


Fig. 10 Zinc atomic electrostatic charge

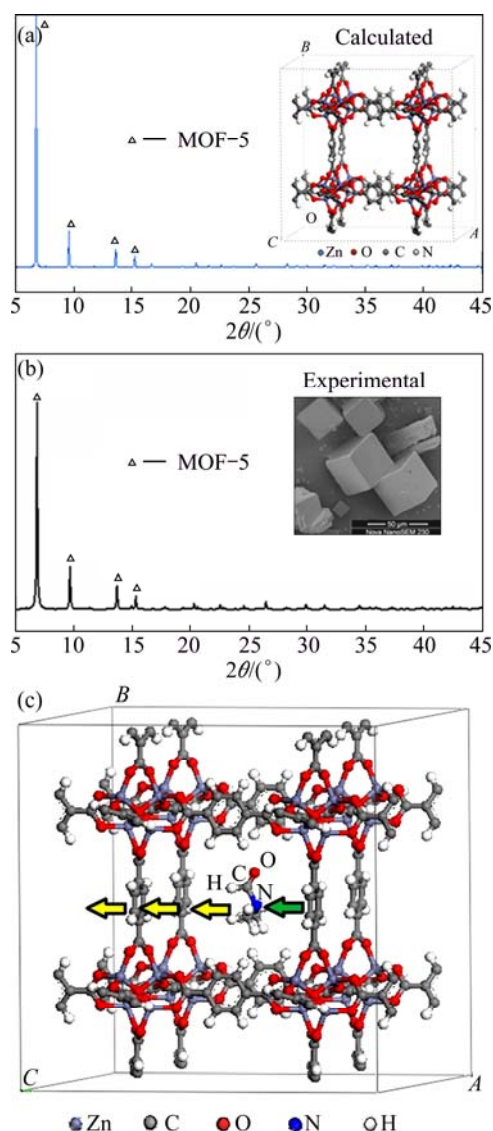


Fig. 11 Theoretical (a) and experimental (b) XRD patterns of $Zn_4O(BDC)_3$ and example of crystal calculation model with DMF (c)

Zn atomic charges in Zn4-NMP-2 and Zn4-DEF-2 were higher, which meant that when the C=O bond was close to Zn group, not only the energy state was not stable mentioned above, but also the electrostatic repulsion effect between $Zn_4O(BDC)_3$ and solvent was more significant and NMP or DEF was easy to remove from framework than DMF.

The energy state and zinc atomic electrostatic charge calculation results explained why DMF was relatively difficult to remove from framework than NMP on microscopic level.

3.7 Energy curves of $[Zn_4O(BDC)_3]_8$ crystal models with NMP, DMF or DEF

For the purpose of study on interaction of solvent molecular in MOF-5 crystal, the crystal model $[Zn_4O(BDC)_3]_8$ with solvent molecular in pore channel

was built. The energy state and electronic structure were calculated using DMol3 program with GGA-BLYP function and DN basis set. The value of the convergence threshold for the maximum energy change was 4.36×10^{-22} J.

Crystal cell model of $[\text{Zn}_4\text{O}(\text{BDC})_3]_8$ represented as MOF-5 was built and the cell parameters were $a=b=c=26.00$ Å, it belonged to P_1 point group of cubic crystal system (see Fig. 11). The theoretical XRD results were well coincident with experimental data, which made sure that the calculation model was reasonable.

Three different solvents, DMF, NMP and DEF, were put in pore centre of $[\text{Zn}_4\text{O}(\text{BDC})_3]_8$ crystal cell as an initial position respectively and denoted as MOF5-DMF, MOF5-NMP and MOF5-DEF. Based on the fraction coordinate of N atom of solvent molecule, Y and Z

fraction coordinates were fixed and solvent molecule moved in pore of framework by X fraction coordinate. Figure 11 also gives the schematic diagram of calculation model taken MOF5-DMF for example and fraction coordinates of N atom of the three models are listed in Table 2.

Energy curves of MOF5-NMP, MOF5-DMF and MOF5-DEF crystal models shown in Fig. 12 (X axis is fraction coordinate of nitrogen atom and nitrogen is in the central of the framework when $X=0.5$) demonstrated that three energy curves were at a minimum when $X=0.2$, which clarified that energy state gradually became more stable when solvent molecule was close to the pore border from centre of the framework. It advised that solvent should be more difficult to remove from border of the framework due to its stable energy state.

Table 2 Fraction coordinate of nitrogen atom of $\text{Zn}_4\text{O}(\text{BDC})_3$ with DMF, NMP or DEF

MOF5-NMP			MOF5-DMF			MOF5-DEF		
X	Y	Z	X	Y	Z	X	Y	Z
0.48193	0.49793	0.49429	0.53153	0.48269	0.49604	0.51491	0.50663	0.50454
0.44804	0.49793	0.49429	0.50376	0.48269	0.49604	0.44184	0.50663	0.50454
0.39576	0.49793	0.49429	0.44539	0.48269	0.49604	0.39185	0.50663	0.50454
0.36388	0.49793	0.49429	0.40259	0.48269	0.49604	0.26134	0.50663	0.50454
0.21593	0.49793	0.49429	0.27774	0.48269	0.49604	0.18636	0.50663	0.50454
0.11673	0.49793	0.49429	0.20395	0.48269	0.49604	0.13082	0.50663	0.50454
			0.11868	0.48269	0.49604			

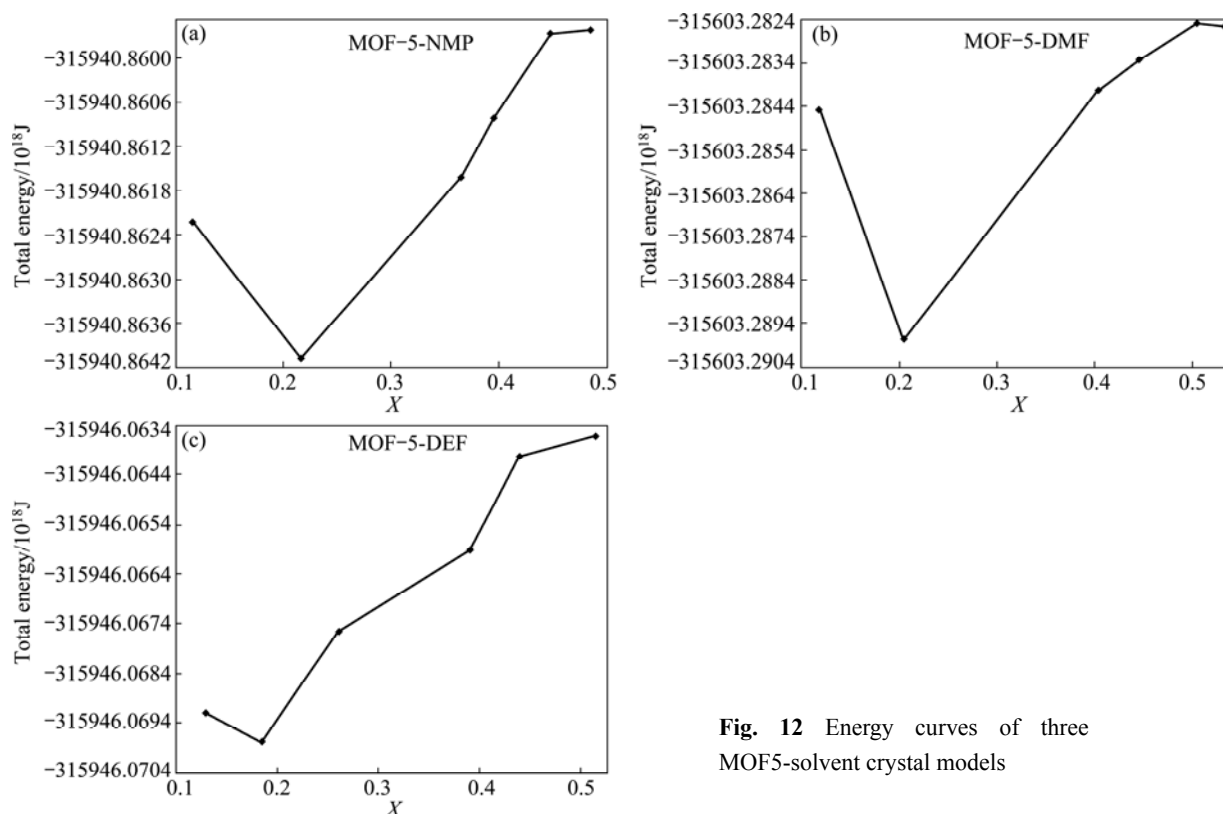


Fig. 12 Energy curves of three MOF5-solvent crystal models

In order to analyze dissolvent process of three different MOF5-solvent crystal models, $\Delta E_{(\text{MOF5-MOF5}^*)} = E_{\text{MOF5}} - (E_{(\text{<MOF5-solvent>})} - E_{\text{solvent}})$ were calculated (see Fig. 13). $\Delta E_{(\text{MOF5-MOF5}^*)}$ was positive value which implied that every dissolvent process mentioned here was possible and three solvents were all suitable for synthesis MOF-5 materials based on the view of favourable energy state. Comparably, $\Delta E_{(\text{MOF5-MOF5}^*)}$ values of MOF5-DEF and MOF5-DMF were the maximum and minimum respectively, which suggested that DMF should be the most difficult to remove from framework compared with NMP and DEF.

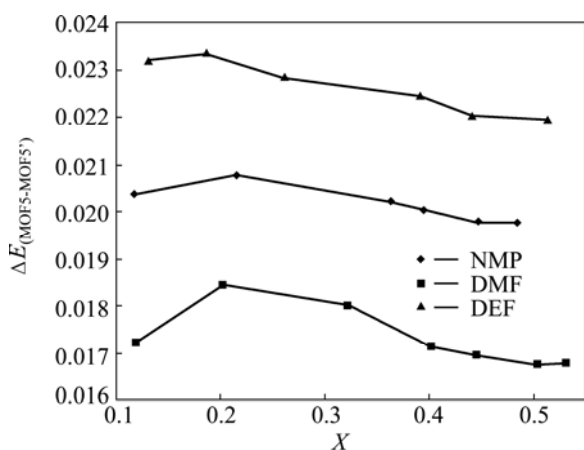


Fig. 13 $\Delta E_{(\text{MOF5-MOF5}^*)}$ curves of three MOF5-Solvent crystal models

4 Conclusions

1) XRD, SEM, TG and FT-IR results indicate that the absorbability of NMP in the pores of $[\text{Zn}_4\text{O}(\text{BDC})_3]_8$ is not stronger than that of DMF, and the thermal stability of $[\text{Zn}_4\text{O}(\text{BDC})_3]_8$ synthesized in DMF is higher than that in NMP. It can be concluded that NMP molecule is easier to move out of the framework than DMF.

2) The nitrogen sorption isotherms present that $[\text{Zn}_4\text{O}(\text{BDC})_3]_8$ prepared using solvent NMP will be favorable to improve gas sorption property and its Langmuir surface area is larger than using DMF.

3) The COSMO solvation model optimized calculations show that the total energy of $\text{Zn}_4\text{O}(\text{BDC})_3$ in NMP is higher than that in DMF and the difference value is 8.6405 kJ/mol. The bonding force between $\text{Zn}_4\text{O}(\text{BDC})_3$ and DMF molecule is stronger and the ionic between zinc and oxygen is reduced because of the effect of solvent.

4) Interaction of $[\text{Zn}_4\text{O}(\text{BDC})_3]_8$ crystal model and solvent molecule DMF, NMP or DEF investigated by DFT methods suggests that the stability of materials synthesized in NMP is lower, and NMP should be easier to be removed from pore of materials compared with

DMF from the point of view of energy state.

References

- KEPERT C J, ROSSEINSKY M J. Zeolite-like crystal structure of an empty microporous molecular framework [J]. *Chemical Communications*, 1999, 35(4): 375–376.
- TSAO C S, YU M S, CHUNG T Y, WU H C, WANG C Y, CHANG K S, CHEN H L. Characterization of pore structure in metal-organic framework by small-angle X-ray scattering [J]. *Journal of the American Chemical Society*, 2007, 129: 15997–16001.
- NELSON A P, FARHA O K, MULFORT K L, HUPP J T. Supercritical processing as a route to high internal surface areas and permanent microporosity in metal-organic frameworks [J]. *Journal of the American Chemical Society*, 2008, 131: 458–460.
- VAIDYANATHAN R, NATARAJAN S, RAO C N R. Unusual dual role of the organic amine in an open framework structure [J]. *Journal of Materials Chemistry*, 1999, 9: 2789–2795.
- VAIDYANATHAN R, NATARAJAN S, CHEETHAM A K, RAO C N R. New open-framework zinc oxalates synthesized in the presence of structure-directing amines [J]. *Chemistry of Materials*, 1999, 11: 3636–3642.
- CASTILLO J M, VLUGT T J H, CALERO S. Understanding water adsorption in Cu-BTC metal-organic frameworks [J]. *Journal of Physical Chemistry C*, 2008, 112: 15934–15939.
- LI H, EDDAOUDI M, O'KEEFFE M, YAGHI O M. Design and synthesis of an exceptionally stable and highly porous metal-organic framework [J]. *Nature*, 1999, 402: 276–279.
- CHEN Chi, PANG Jun, HAN Shuang, ZHANG Bi-xia, HUANG Yuan, MIAO Ling, JIANG Jian-jun. Influence of functional group decoration on C in MOF-5 [J]. *Acta Physico-Chimica Sinica*, 2012, 28(1): 189–194. (in Chinese)
- ZHAO Nan, DENG Hong-ping, SHU Mou-hai. Preparation and catalytic performance of Pd catalyst supported on MOF-5 [J]. *Chinese Journal of Inorganic Chemistry*, 2010(7): 1213–1217. (in Chinese)
- YANG Ru, LIU Yuan-bin, LIU Guo-qiang, LI Min. Porous structure analysis of terephthalic acid-zinc complex [J]. *Chinese Journal of Inorganic Chemistry*, 2008, 24(12): 1962–1969. (in Chinese)
- LI Y, YANG R T. Significantly enhanced hydrogen storage in metal-organic-frameworks via spillover [J]. *Journal of the American Chemical Society*, 2005, 128(3): 726–727.
- CHENG S, LIU S, ZHAO Q. Improved synthesis and hydrogen storage of a micro-porous metal-organic framework material [J]. *Energy Conversion and Management*, 2009, 50(5): 1314–1317.
- ZHAO Z, MA X, LI Z, LIN Y S. Synthesis, characterization and gas transport properties of MOF-5 membranes [J]. *Journal of Membrane Science*, 2011, 382(1–2): 82–90.
- KIM H, DAS S, KIM M G, DYBTSEV D N, KIM Y, KIM K. Synthesis of phase-pure interpenetrated MOF-5 and its gas sorption properties [J]. *Inorganic Chemistry*, 2011, 50(8): 3691–3696.
- ROSI N L, ECKERT J, EDDAOUDI M, VODAK D T, KIM J, O'KEEFFE M, YAGHI O M. Hydrogen storage in microporous metal-organic frameworks [J]. *Science*, 2003, 300(5622): 1127–1129.
- ROSI N L, EDDAOUDI M, KIM J. Infinite secondary building units and forbidden catenation in metal-organic frameworks [J]. *Angewandte Chemie*, 2002, 114(2): 294–297.
- SABO M, HENSCHER A, FRÖDE H. Solution infiltration of palladium into MOF-5: Synthesis, physisorption and catalytic properties [J]. *Journal of Materials Chemistry*, 2007, 17(36): 3827–3832.
- ZHANG L, HU Y H. Desorption of dimethylformamide from

- Zn₄O(C₈H₄O₄)₃ framework [J]. Applied Surface Science, 2011, 257(8): 3392–3398
- [19] SON W J, KIM J, JAHEON K, AHN W S. Sonochemical synthesis of MOF-5 [J]. Chemical Communications, 2008, 40: 6336–6338.
- [20] LU C M, LIU J, XIAO K. Microwave enhanced synthesis of MOF-5 and its CO₂ capture ability at moderate temperatures across multiple capture and release cycles [J]. Chemical Engineering Journal, 2010, 156(2): 465–470.
- [21] LEE S Y, PARK S J. Effect of platinum doping of activated carbon on hydrogen storage behaviors of metal-organic frameworks-5 [J]. International Journal of Hydrogen Energy, 2011, 36(14): 8381–8387.
- [22] HAUSDORF S, BAITALOW F, SEIDEL J. Gaseous species as reaction tracers in the solvothermal synthesis of the zinc oxide terephthalate MOF-5 [J]. The Journal of Physical Chemistry A, 2007, 111(20): 4259–4266.
- [23] YAGHI O M, LI H L, DAVIS C, RICHARDSON D, GROU T L. Synthetic strategies, structure patterns, and emerging properties in the chemistry of modular porous [J]. Accounts of Chemical Research, 1998, 31: 474–484.
- [24] STALLMACH F, GRÖGER S, KÜNZEL V, KÄRGER J, YAGHI O M, HESSE M, MÜLLER U. MR studies on the diffusion of hydrocarbons on the metal-organic framework material MOF-5 [J]. Angewandte Chemie International Edition, 2006, 45: 2123–2126.
- [25] ZHANG L, HU Y H. A systematic investigation of decomposition of nano Zn₄O(C₈H₄O₄)₃ metal-organic framework [J]. The Journal of Physical Chemistry C, 2010, 114: 2566–2571.
- [26] PANELLA B, HIRSCHER M, PUTTER H, MULLER U. Hydrogen adsorption in metal-organic frameworks: Cu-MOFs and Zn-MOFs compared [J]. Advanced Functional Materials, 2006, 16: 520–524.
- [27] HUANG L, WANG H, CHEN J, WANG Z, SUN J, ZHAO D, YAN Y. Synthesis, morphology control and properties of porous metal-organic coordination polymers [J]. Microporous Mesoporous Materials, 2003, 58: 105–114.
- [28] EDDAOUDI M, KIM J, ROSI N, VODAK D, WACHTER J, O'KEEFFE M, YAGHI O M. Systematic design of pore size and functionality in isorecticular MOFs and their application in methane storage [J]. Science, 2002, 295(5554): 469–472.
- [29] ZHAO Z, LI Z, LIN Y S. Adsorption and diffusion of carbon dioxide on metal-organic framework (MOF-5) [J]. Industrial & Engineering Chemistry Research, 2009, 48: 10015–10020.
- [30] HAFIZOVIC J, BJORGEN M, OLSBYE U, DIETZEL P D C, BORDIGA S, PRESTIPINO C, LAMBERTI C, LILLERUD K P. The inconsistency in adsorption properties and powder XRD data of MOF-5 is rationalized by framework interpenetration and the presence of organic and inorganic species in the nanocavities [J]. Journal of the American Chemical Society, 2007, 129: 3612–3616.
- [31] KLAMT A, SCHÜRMANN G. COSMO: A new approach to dielectric screening in solvents with explicit expressions for the screening energy and its gradient [J]. Journal of Chemical Society, 1993, 2: 799–804.
- [32] KLAMT A, JONAS V, BURGER T, LOHRENZ J. Refinement and parametrization of COSMO-RS [J]. The Journal of Physical Chemistry, 1998, 102: 5074–5080.
- [33] DELLEY B. The conductor-like screening model for polymers and surfaces [J]. Molecular Simulation, 2006, 32: 117–123.
- [34] DELLEY B. Ground-state enthalpies: Evaluation of electronic structure approaches with emphasis on the density functional method [J]. The Journal of Physical Chemistry A, 2006, 110: 13632–13639.
- [35] DELLEY B. Time dependent density functional theory with DMol3 [J]. Journal of Physics: Condensed Matter, 2010, 22: 38420–38426.

NMP/DMF 对溶剂热法合成[Zn₄O(BDC)₃]₈ 的影响及框架-溶剂相互作用机制

吴争平^{1,2}, 王明雪¹, 周丽姣¹, 尹周澜^{1,2}, 谈进¹, 张锦玲¹, 陈启元^{1,2}

1. 中南大学 化学化工学院, 长沙 410083;

2. 中南大学 教育部有色金属资源化学重点实验室, 长沙 410083

摘要: 为探究溶剂对合成有机金属框架化合物的影响机制, 采用实验和 DFT 理论计算相结合的方法, 研究溶剂 N,N-二甲基甲酰胺(DMF)和 N-甲基-2-吡咯烷酮(NMP)对溶剂热法合成有机金属框架材料[Zn₄O(BDC)₃]₈ 的影响及溶剂与框架间的微观作用机制。粉末 X 射线衍射(XRD)和扫描电镜(SEM)结果表明, NMP 在[Zn₄O(BDC)₃]₈ 孔道中的吸附力较 DMF 的弱, NMP 分子更容易从框架中脱除; 热重(TG)和热重-红外联用(TGA/FT-IR)结果表明, 以 DMF 为溶剂合成的[Zn₄O(BDC)₃]₈ 的热分解温度和热稳定性较高; 氮气等温吸附实验(BET)发现, 以 NMP 为溶剂合成的[Zn₄O(BDC)₃]₈ 的气体吸附性能更强, 兰缪尔比表面积高于用 DMF 合成的[Zn₄O(BDC)₃]₈。调控介电常数设定溶剂分别为 NMP 和 DMF, 用 COSMO 溶剂化方法对溶剂分子与框架化合物基本结构单元 Zn₄O(BDC)₃ 间相互作用模型进行几何优化计算, 发现溶剂设定为 NMP 时 Zn₄O(BDC)₃ 优化结构的总能量较溶剂设定为 DMF 时的高 8.6405 kJ/mol, 这说明 DMF 分子与 Zn₄O(BDC)₃ 间的结合力强于 NMP 分子的, 溶剂化作用降低了 Zn 与 O 间的离子性; 用 DMol3 在 GGA-BLYP/ DN 水平计算了 DMF、NMP 或 DEF 溶剂分子在[Zn₄O(BDC)₃]₈ 晶体孔道中的相互作用, 与 DMF 相比, NMP 在孔道中能量状态稳定性较差, 在能量状态角度上 NMP 应最容易从框架材料孔道中脱除。研究结果说明 NMP 更有利于合成性质良好的[Zn₄O(BDC)₃]₈, 与 DMF 相比 NMP 与框架结构基元间的作用力较弱。

关键词: 溶剂热合成; [Zn₄O(BDC)₃]₈; N-甲基-2-吡咯烷酮; 相互作用机制; COSMO 溶剂化模型; 密度泛函方法

(Edited by Xiang-qun LI)